

STERILE NEUTRINO FITS

CARLO GIUNTI

INFN, Sezione di Torino, Via P. Giuria 1, I-10125 Torino, Italy

ABSTRACT

After a brief review of the results of solar, atmospheric and long-baseline neutrino oscillation experiments which led to the current three-neutrino mixing paradigm, we discuss indications of neutrino oscillation experiments in favor of short-baseline oscillations which require the existence of one or more sterile neutrinos. We show that the simplest possibility of existence of one sterile neutrino is not enough to fit all data of short-baseline neutrino oscillation experiments because of two tensions: a tension between neutrino and antineutrino data and a tension between appearance and disappearance data. The tension between neutrino and antineutrino data is eliminated with the addition of a second sterile neutrino which allows CP-violating effects in short-baseline experiments. In this case the tension between appearance and disappearance data is reduced, but cannot be eliminated.

1. Introduction: Three-Neutrino Mixing Paradigm

The results of several solar, atmospheric and long-baseline neutrino oscillation experiment have proved that neutrinos are massive and mixed particles (see Ref. [1]). There are two groups of experiments which measured two independent squared-mass differences (Δm^2) in two different neutrino flavor transition channels.

Solar neutrino experiments (Homestake, Kamiokande, GALLEX/GNO, SAGE, Super-Kamiokande, SNO, BOREXino) measured $\nu_e \rightarrow \nu_\mu, \nu_\tau$ oscillations generated by $\Delta m_{\text{SOL}}^2 = 6.2_{-1.9}^{+1.1} \times 10^{-5} \text{ eV}^2$ and a mixing angle $\tan^2 \vartheta_{\text{SOL}} = 0.42_{-0.02}^{+0.04}$ [2]. The KamLAND experiment confirmed these oscillations by observing the disappearance of reactor $\bar{\nu}_e$ at an average distance of about 180 km. The combined fit of solar and KamLAND data leads to $\Delta m_{\text{SOL}}^2 = (7.6 \pm 0.2) \times 10^{-5} \text{ eV}^2$ and a mixing angle $\tan^2 \vartheta_{\text{SOL}} = 0.44 \pm 0.03$ [2]. Notice that the agreement of solar and KamLAND data in favor of ν_e and $\bar{\nu}_e$ disappearance generated by the same oscillation parameters is consistent with the equality of neutrino and antineutrino disappearance expected from CPT symmetry (see Ref. [1]).

Atmospheric neutrino experiments (Kamiokande, IMB, Super-Kamiokande, MACRO, Soudan-2, MINOS) measured ν_μ and $\bar{\nu}_\mu$ disappearance through oscillations generated by $\Delta m_{\text{ATM}}^2 \simeq 2.3 \times 10^{-3} \text{ eV}^2$ and a mixing angle $\sin^2 2\vartheta_{\text{ATM}} \simeq 1$ [3]. The K2K and MINOS long-baseline experiments confirmed these oscillations by observing the disappearance of accelerator ν_μ at distances of about 250 km and 730 km, respectively. The MINOS data give $\Delta m_{\text{ATM}}^2 = 2.32_{-0.08}^{+0.12} \times 10^{-3} \text{ eV}^2$ and $\sin^2 2\vartheta_{\text{ATM}} > 0.90$ at 90% C.L. [4]. The equality of muon neutrino and antineutrino disappearance expected from CPT symmetry is currently under investigation in the MINOS experiment [5],

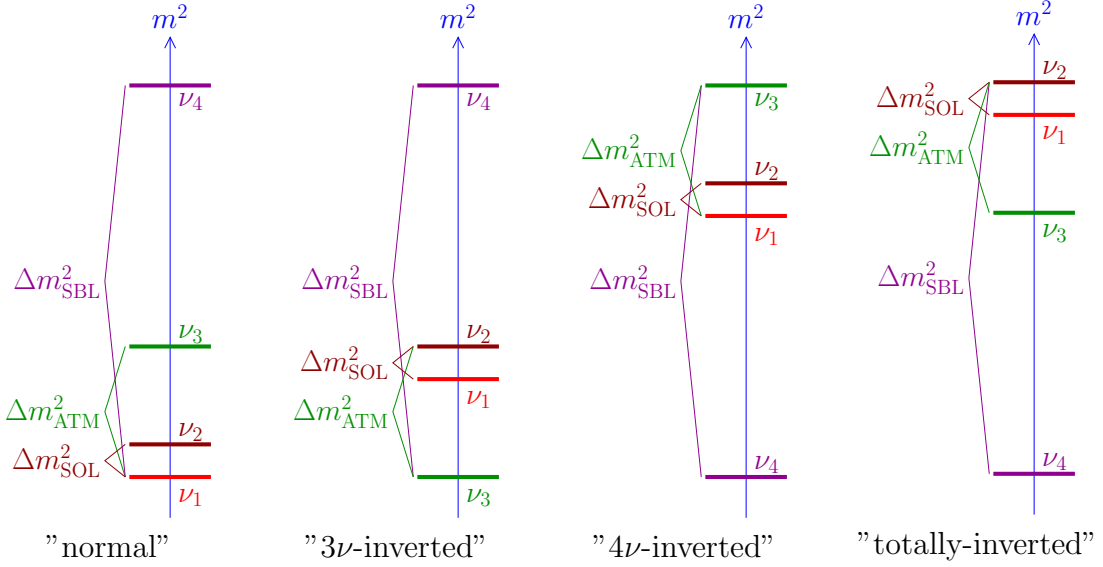


Figure 1: 3+1 four-neutrino schemes.

with preliminary results which hint at an intriguing difference between the muon neutrino and antineutrino oscillation parameters.

These measurements led to the current three-neutrino mixing paradigm, in which the three active neutrinos ν_e , ν_μ , ν_τ are superpositions of three massive neutrinos ν_1 , ν_2 , ν_3 with respective masses m_1 , m_2 , m_3 . The two measured squared-mass differences can be interpreted as

$$\Delta m_{\text{SOL}}^2 = \Delta m_{21}^2, \quad \Delta m_{\text{ATM}}^2 = |\Delta m_{31}^2| \simeq |\Delta m_{32}^2|, \quad (1)$$

with $\Delta m_{kj}^2 = m_k^2 - m_j^2$. In the standard parameterization of the 3×3 unitary mixing matrix (see Ref. [1]) $\vartheta_{\text{SOL}} \simeq \vartheta_{12}$, $\vartheta_{\text{ATM}} \simeq \vartheta_{23}$ and $\sin^2 \vartheta_{13} < 0.035$ at 90% C.L. [6].

The completeness of the three-neutrino mixing paradigm has been challenged by the recent observation of a signal of short-baseline $\bar{\nu}_\mu \rightarrow \bar{\nu}_e$ oscillations in the MiniBooNE experiment [7] which agrees with a similar signal observed several years ago in the LSND experiment [8]. It is remarkable that the two signals have been observed at different values of distance (L) and energy (E), but approximately at the same L/E . Since the distance and energy dependences of neutrino oscillations occur through this ratio, the agreement of the MiniBooNE and LSND signals raised interest in the possibility of existence of one or more squared-mass differences much larger than Δm_{SOL}^2 and Δm_{ATM}^2 . These new squared-mass differences should have values larger than about 0.5 eV.

2. 3+1 Neutrino Mixing

In the following, I consider first the simplest extension of three-neutrino mixing with the addition of one massive neutrino. In such four-neutrino mixing framework

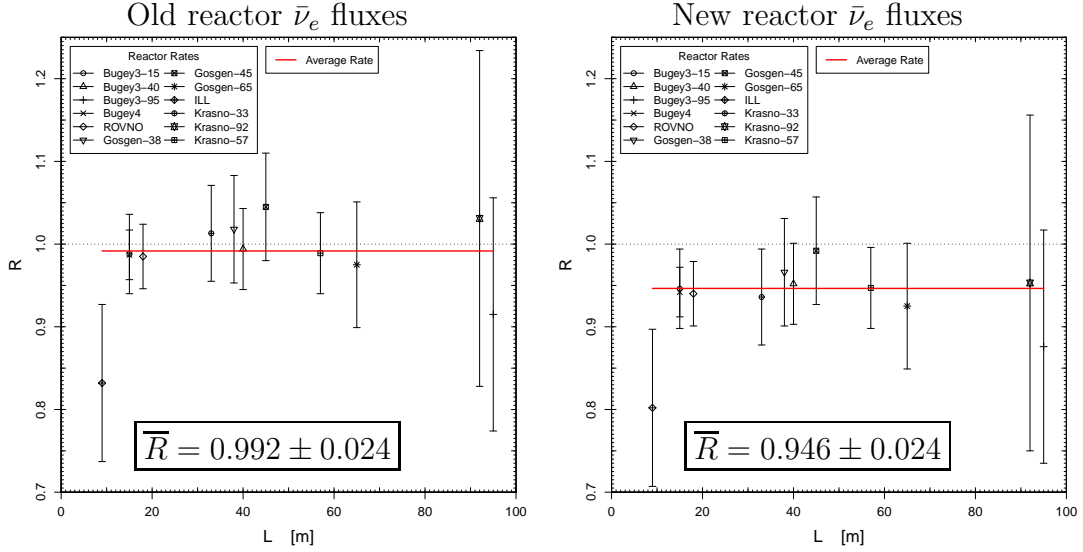


Figure 2: Ratio R of the observed $\bar{\nu}_e$ event rate and that expected in absence of $\bar{\nu}_e$ disappearance obtained from the old (see Ref. [14]) and new [15] reactor $\bar{\nu}_e$ fluxes. The average value of R obtained with the new reactor $\bar{\nu}_e$ fluxes quantifies the reactor antineutrino anomaly [16].

the flavor neutrino basis is composed by the three active neutrinos ν_e , ν_μ , ν_τ and a sterile neutrino ν_s which does not have weak interactions and does not contribute to the invisible width of the Z boson [9]. The existence of sterile neutrinos which have been thermalized in the early Universe is compatible with Big-Bang Nucleosynthesis data [10, 11] and cosmological measurements of the Cosmic Microwave Background and Large-Scale Structures if the mass of the fourth neutrino is limited below about 1 eV [12, 13].

So-called 2+2 four-neutrino mixing schemes are strongly disfavored by the absence of any signal of sterile neutrino effects in solar and atmospheric neutrino data [17]. Hence, we must consider the so-called 3+1 four-neutrino schemes depicted in Fig. 1. Since the "4 ν -inverted" and "totally-inverted" schemes have three massive neutrinos at the eV scale, they are disfavored by cosmological data over the "normal" and "3 ν -inverted" schemes. In all 3+1 schemes the effective flavor transition and survival probabilities in short-baseline (SBL) experiments are given by

$$P_{\nu_\alpha \rightarrow \nu_\beta}^{\text{SBL}(-)} = \sin^2 2\vartheta_{\alpha\beta} \sin^2 \left(\frac{\Delta m^2 L}{4E} \right) \quad (\alpha \neq \beta), \quad (2)$$

$$P_{\nu_\alpha \rightarrow \nu_\alpha}^{\text{SBL}} = 1 - \sin^2 2\vartheta_{\alpha\alpha} \sin^2 \left(\frac{\Delta m^2 L}{4E} \right), \quad (3)$$

for $\alpha, \beta = e, \mu, \tau, s$, with $\Delta m^2 = \Delta m_{\text{SBL}}^2$ and

$$\sin^2 2\vartheta_{\alpha\beta} = 4|U_{\alpha 4}|^2 |U_{\beta 4}|^2, \quad (4)$$

$$\sin^2 2\vartheta_{\alpha\alpha} = 4|U_{\alpha 4}|^2 (1 - |U_{\alpha 4}|^2). \quad (5)$$

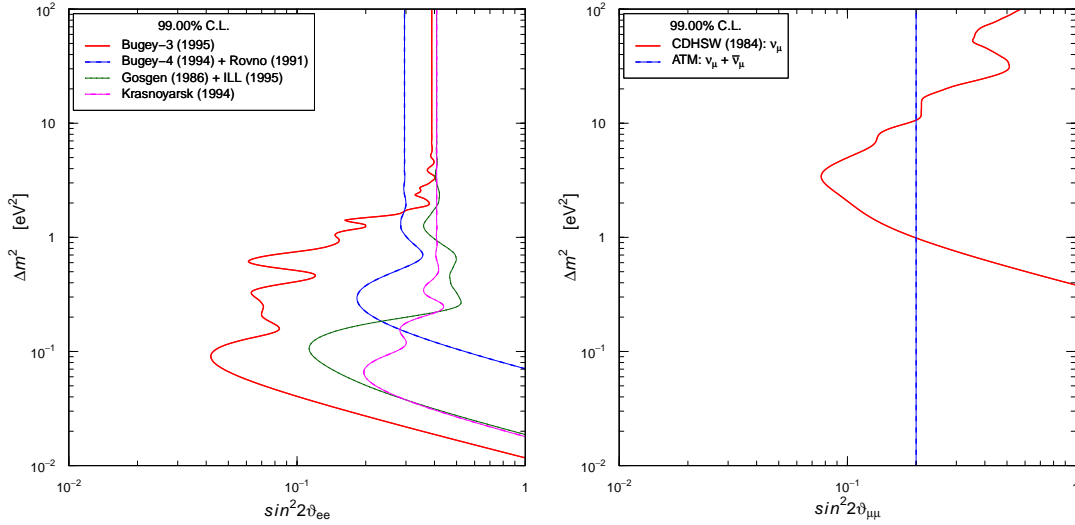


Figure 3: Exclusion curves obtained from the data of reactor $\bar{\nu}_e$ disappearance experiments (see Ref. [16]), from the data of the CDHSW ν_μ disappearance experiment [18], and from atmospheric neutrino data (extracted from the analysis in Ref. [19]).

Therefore:

1. All effective SBL oscillation probabilities depend only on the largest squared-mass difference $\Delta m^2 = \Delta m_{\text{SBL}}^2 = |\Delta m_{41}^2|$.
2. All oscillation channels are open, each one with its own oscillation amplitude.
3. All oscillation amplitudes depend only on the absolute values of the elements in the fourth column of the mixing matrix, i.e. on three real numbers with sum less than unity, since the unitarity of the mixing matrix implies $\sum_\alpha |U_{\alpha 4}|^2 = 1$
4. CP violation cannot be observed in SBL oscillation experiments, even if the mixing matrix contains CP-violation phases. In other words, neutrinos and antineutrinos have the same effective SBL oscillation probabilities.

Before the recent indication of an antineutrino $\bar{\nu}_\mu \rightarrow \bar{\nu}_e$ signal consistent with the LSND antineutrino signal, the MiniBooNE collaboration published the results of neutrino data which do not show a corresponding $\nu_\mu \rightarrow \nu_e$ signal [20]. This difference between the MiniBooNE neutrino and antineutrino data may be due to CP violation.

The absence of any difference in the effective SBL oscillation probabilities of neutrinos and antineutrinos in 3+1 four-neutrino mixing schemes implies that these schemes cannot explain the difference between neutrinos and antineutrino oscillations observed in the MiniBooNE. Moreover, the dependence of all the oscillation amplitudes in Eqs. (4) and (5) on three independent absolute values of the elements in the fourth column of the mixing matrix implies that the amplitude of $\bar{\nu}_\mu^{(-)} \rightarrow \bar{\nu}_e^{(-)}$ transitions

is limited by the absence of large SBL disappearance of $\bar{\nu}_e$ and $\bar{\nu}_\mu$ observed in several experiments.

The results of reactor neutrino experiments constrain the value $|U_{e4}|^2$ through the measurement of $\sin^2 2\vartheta_{ee}$. The calculation of the reactor $\bar{\nu}_e$ flux has been recently improved in Ref. [15], resulting in an increase of about 3% with respect to the previous value adopted by all experiments for the comparison with the data. As illustrated in Fig. 2, the measured reactor rates are in agreement with those derived from the old $\bar{\nu}_e$ flux, but show a deficit of about 2.2σ with respect to the rates derived from the new $\bar{\nu}_e$ flux. This is the ‘‘reactor antineutrino anomaly’’ [16]^a, which may be an indication in the $\bar{\nu}_e \rightarrow \bar{\nu}_e$ channel of a signal corresponding to the $\bar{\nu}_\mu \rightarrow \bar{\nu}_e$ signal observed in the LSND and MiniBooNE experiments. However, the $\bar{\nu}_e$ disappearance is small and large values of $\sin^2 2\vartheta_{ee}$ are constrained by the exclusion curves in the left panel of Fig. 3. Since values of $|U_{e4}|^2$ close to unity are excluded by solar neutrino oscillations (which require large $|U_{e1}|^2 + |U_{e2}|^2$), for small $\sin^2 2\vartheta_{ee}$ we have

$$\sin^2 2\vartheta_{ee} \simeq 4|U_{e4}|^2. \quad (6)$$

The value of $\sin^2 2\vartheta_{\mu\mu}$ is constrained by the curves in the right panel of Fig. 3, which have been obtained from the lack of ν_μ disappearance in the CDHSW ν_μ experiment [18] and from the requirement of large $|U_{\mu1}|^2 + |U_{\mu2}|^2 + |U_{\mu3}|^2$ for atmospheric neutrino oscillations [19]. Hence, $|U_{\mu4}|^2$ is small and

$$\sin^2 2\vartheta_{\mu\mu} \simeq 4|U_{\mu4}|^2. \quad (7)$$

From Eqs. (4), (6) and (7), for the amplitude of $\bar{\nu}_\mu \rightarrow \bar{\nu}_e$ transitions we obtain

$$\sin^2 2\vartheta_{e\mu} \simeq \frac{1}{4} \sin^2 2\vartheta_{ee} \sin^2 2\vartheta_{\mu\mu}. \quad (8)$$

Therefore, if $\sin^2 2\vartheta_{ee}$ and $\sin^2 2\vartheta_{\mu\mu}$ are small, $\sin^2 2\vartheta_{e\mu}$ is quadratically suppressed. This is illustrated in the left panel of Fig. 4, where one can see that the separate effects of the constraints on $\sin^2 2\vartheta_{ee}$ and $\sin^2 2\vartheta_{\mu\mu}$ exclude only the large- $\sin^2 2\vartheta_{e\mu}$ part of the region allowed by LSND and MiniBooNE antineutrino data, whereas most of this region is excluded by the combined constraint in Eq. (8). As shown in the right panel of Fig. 4, the constraint becomes stronger by including the data of the KARMEN [27], NOMAD [28] and MiniBooNE neutrino [20] experiments, which did not observe a short-baseline $\bar{\nu}_\mu \rightarrow \bar{\nu}_e$ signal. Since the parameter goodness-of-fit [29] is 0.0016%, 3+1 schemes are strongly disfavored by the data. This conclusion has been reached recently also in Refs. [19, 30–32] and confirms the pre-MiniBooNE results in Refs. [17, 33].

^a We do not consider here the ‘‘Gallium neutrino anomaly’’ [21–26], which may be compatible with the reactor antineutrino anomaly assuming the equality of neutrino and antineutrino disappearance imposed by the CPT symmetry.

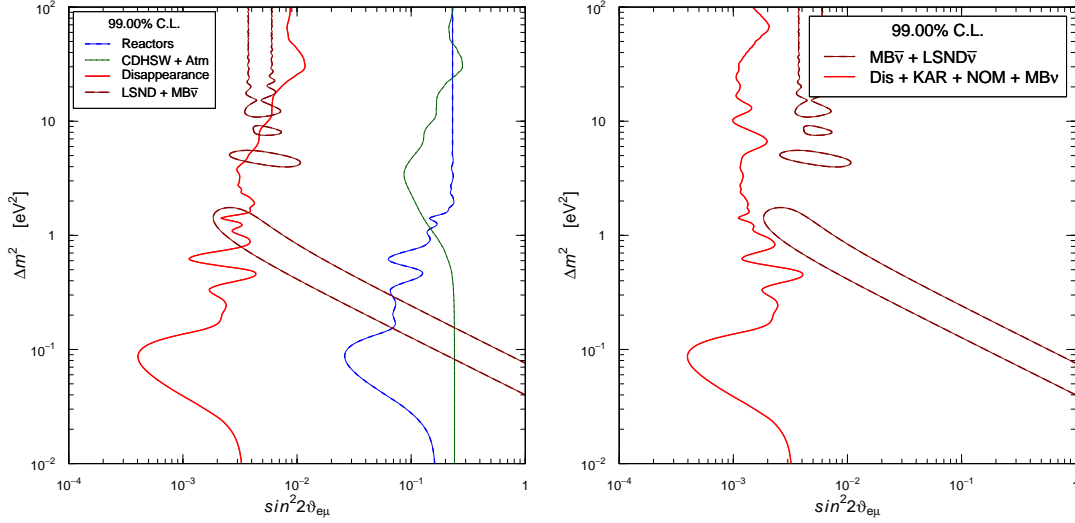


Figure 4: Left Panel: Exclusion curves in the $\sin^2 2\theta_{e\mu}-\Delta m^2$ plane obtained from the separate constraints in Fig. 3 (blue and green lines) and the combined constraint given by Eq. (8) (red line) from disappearance experiments (Dis). Right Panel: Exclusion curve obtained with the addition of KARMEN [27] (KAR), NOMAD [28] (NOM) and MiniBooNE neutrino [20] ($MB\nu$) data (red line). In both panels the region enclosed by the dark-red lines is allowed by LSND and MiniBooNE antineutrino data.

The CP-violating difference between MiniBooNE neutrino and antineutrino data can be explained by introducing another physical effect in addition to a sterile neutrino: a second sterile neutrino in 3+2 schemes [19, 30, 32, 34–36], non-standard interactions [30], CPT violation [31, 37]. In the following I discuss the possibility of 3+2 neutrino mixing.

3. 3+2 Neutrino Mixing

In 3+2 schemes the relevant effective oscillation probabilities in short-baseline experiments are given by

$$P_{\nu_{\mu} \rightarrow \nu_e}^{\text{SBL}(-)} = 4|U_{\mu 4}|^2|U_{e 4}|^2 \sin^2 \phi_{41} + 4|U_{\mu 5}|^2|U_{e 5}|^2 \sin^2 \phi_{51} \quad (9)$$

$$+ 8|U_{\mu 4}U_{e 4}U_{\mu 5}U_{e 5}| \sin \phi_{41} \sin \phi_{51} \cos(\phi_{54}^{(+)} - \eta),$$

$$P_{\nu_{\alpha} \rightarrow \nu_{\alpha}}^{\text{SBL}} = 1 - 4(1 - |U_{\alpha 4}|^2 - |U_{\alpha 5}|^2)(|U_{\alpha 4}|^2 \sin^2 \phi_{41} + |U_{\alpha 5}|^2 \sin^2 \phi_{51}) \quad (10)$$

$$+ 4|U_{\alpha 4}|^2|U_{\alpha 5}|^2 \sin^2 \phi_{54},$$

for $\alpha, \beta = e, \mu$, with

$$\phi_{kj} = \Delta m_{kj}^2 L/4E, \quad \eta = \arg[U_{e 4}^* U_{\mu 4} U_{e 5} U_{\mu 5}^*]. \quad (11)$$

Note the change in sign of the contribution of the CP-violating phase η going from

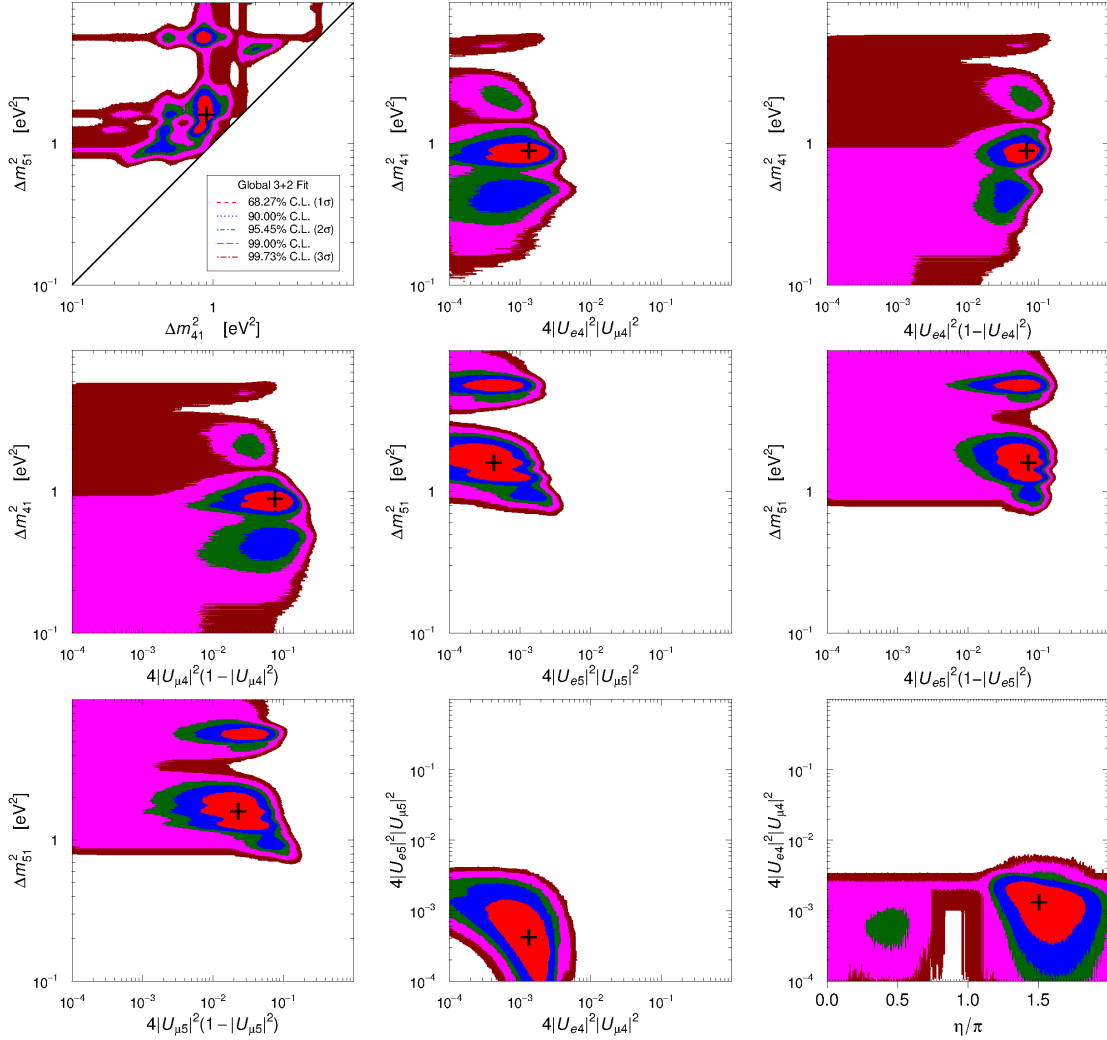


Figure 5: Marginal allowed regions in two-dimensional planes of interesting combinations of the oscillation parameters in 3+2 neutrino mixing.

neutrinos to antineutrinos, which allows us to explain the CP-violating difference between MiniBooNE neutrino and antineutrino data.

Figure 5 shows the marginal allowed regions in two-dimensional planes of interesting combinations of the oscillation parameters in our 3+2 global fit of the same set of data used in Fig. 4. The best-fit values of the mixing parameters are:

$$\Delta m_{41}^2 = 0.90 \text{ eV}^2, |U_{e4}|^2 = 0.017, |U_{\mu 4}|^2 = 0.019, \quad (12)$$

$$\Delta m_{51}^2 = 1.61 \text{ eV}^2, |U_{e5}|^2 = 0.018, |U_{\mu 5}|^2 = 0.0058, \eta = 1.51\pi. \quad (13)$$

The parameter goodness-of-fit obtained with the comparison of the fit of LSND and MiniBooNE antineutrino data and the fit of all other data is 0.24%. This is an improvement with respect to the 0.0016% parameter goodness-of-fit obtained in 3+1

schemes. However, the value of the parameter goodness-of-fit remains low as a consequence of the fact that the $\bar{\nu}_\mu \rightarrow \bar{\nu}_e$ transitions observed in LSND and MiniBooNE must correspond in any neutrino mixing schemes to enough short-baseline disappearance of $\bar{\nu}_e$ and $\bar{\nu}_\mu$ which has not been observed.

The results of our 3+2 global fit are in reasonable agreement with those presented in Ref. [32]. There is a discrepancy in the location of the best-fit point in the $\Delta m_{41}^2 - \Delta m_{51}^2$ plane, but we obtain similar regions for the local χ^2 minima. Our allowed regions are larger than those presented in Ref. [32]. I think that such difference is probably due to a different treatment of the spectral data of the Bugey-3 reactor experiment [38] which cause the wiggling for $\Delta m^2 \lesssim 1 \text{ eV}^2$ of the disappearance limit in the left panel of Fig. 4 and the exclusion curve in the right panel of Fig. 4. Such wiggling is wider in Fig. 3 of Ref. [32], leading to deeper valleys of the χ^2 function and smaller allowed regions.

4. Conclusions

In conclusion, I think that we are living an exciting time in neutrino physics which may prelude to a transition from the well-established three-neutrino mixing paradigm to a new paradigm of neutrino mixing with sterile neutrinos and possibly other effects (as non-standard interactions and CPT violation) which are very interesting for the exploration of the physics beyond the Standard Model. In order to clarify the validity of the experimental indications in favor of an expansion of neutrino mixing beyond the standard three-neutrino mixing and resolve the tension between the current positive and negative experimental results, new experiments with high sensitivity and low background are needed (see, for example, those proposed in Refs. [39–44]).

5. References

- 1) C. Giunti and C.W. Kim, *Fundamentals of Neutrino Physics and Astrophysics* (Oxford University Press, Oxford, UK, 2007).
- 2) Super-Kamiokande, K. Abe et al., *Phys. Rev. D* **83** (2011) 052010, arXiv:1010.0118.
- 3) Super-Kamiokande, Y. Ashie et al., *Phys. Rev. D* **71** (2005) 112005, hep-ex/0501064.
- 4) MINOS, P. Adamson et al., *Phys. Rev. Lett.* **106** (2011) 181801, arXiv:1103.0340.
- 5) MINOS, P. Adamson et al., (2011), arXiv:1104.0344.
- 6) T. Schwetz, M. Tortola and J.W.F. Valle, *New J. Phys.* **10** (2008) 113011, arXiv:0808.2016.
- 7) MiniBooNE, A.A. Aguilar-Arevalo et al., *Phys. Rev. Lett.* **105** (2010) 181801, arXiv:1007.1150.

- 8) LSND, A. Aguilar et al., Phys. Rev. D64 (2001) 112007, hep-ex/0104049.
- 9) ALEPH, DELPHI, L3, OPAL, SLD, LEP Electroweak Working Group, SLD Electroweak Group, SLD Heavy Flavour Group, S. Schael et al., Phys. Rept. 427 (2006) 257, hep-ex/0509008.
- 10) R.H. Cyburt et al., Astropart. Phys. 23 (2005) 313, astro-ph/0408033.
- 11) Y.I. Izotov and T.X. Thuan, Astrophys. J. 710 (2010) L67, arXiv:1001.4440.
- 12) J. Hamann et al., Phys. Rev. Lett. 105 (2010) 181301, arXiv:1006.5276.
- 13) E. Giusarma et al., (2011), arXiv:1102.4774.
- 14) C. Bemporad, G. Gratta and P. Vogel, Rev. Mod. Phys. 74 (2002) 297, hep-ph/0107277.
- 15) T.A. Mueller et al., (2011), arXiv:1101.2663.
- 16) G. Mention et al., Phys. Rev. D83 (2011) 073006, arXiv:1101.2755.
- 17) M. Maltoni et al., New J. Phys. 6 (2004) 122, hep-ph/0405172.
- 18) CDHSW, F. Dydak et al., Phys. Lett. B134 (1984) 281.
- 19) M. Maltoni and T. Schwetz, Phys. Rev. D76 (2007) 093005, arXiv:0705.0107.
- 20) MiniBooNE, A.A. Aguilar-Arevalo, Phys. Rev. Lett. 102 (2009) 101802, arXiv:0812.2243.
- 21) C. Giunti and M. Laveder, Mod. Phys. Lett. A22 (2007) 2499, hep-ph/0610352.
- 22) C. Giunti and M. Laveder, Phys. Rev. D77 (2008) 093002, arXiv:0707.4593.
- 23) M.A. Acero, C. Giunti and M. Laveder, Phys. Rev. D78 (2008) 073009, arXiv:0711.4222.
- 24) C. Giunti and M. Laveder, Phys. Rev. D80 (2009) 013005, arXiv:0902.1992.
- 25) C. Giunti and M. Laveder, Phys. Rev. D82 (2010) 053005, arXiv:1005.4599.
- 26) C. Giunti and M. Laveder, (2010), arXiv:1006.3244.
- 27) KARMEN, B. Armbruster et al., Phys. Rev. D65 (2002) 112001, hep-ex/0203021.
- 28) NOMAD, P. Astier et al., Phys. Lett. B570 (2003) 19, hep-ex/0306037.
- 29) M. Maltoni and T. Schwetz, Phys. Rev. D68 (2003) 033020, hep-ph/0304176.
- 30) E. Akhmedov and T. Schwetz, JHEP 10 (2010) 115, arXiv:1007.4171.
- 31) C. Giunti and M. Laveder, Phys. Rev. D83 (2011) 053006, arXiv:1012.0267.
- 32) J. Kopp, M. Maltoni and T. Schwetz, (2011), arXiv:1103.4570.
- 33) M. Maltoni et al., Nucl. Phys. B643 (2002) 321, hep-ph/0207157.
- 34) M. Sorel, J. Conrad and M. Shaevitz, Phys. Rev. D70 (2004) 073004, hep-ph/0305255.
- 35) G. Karagiorgi et al., Phys. Rev. D75 (2007) 013011, hep-ph/0609177.
- 36) G. Karagiorgi et al., Phys. Rev. D80 (2009) 073001, arXiv:0906.1997.
- 37) C. Giunti and M. Laveder, Phys. Rev. D82 (2010) 093016, arXiv:1010.1395.
- 38) Bugey, B. Achkar et al., Nucl. Phys. B434 (1995) 503.
- 39) A. Ianni, D. Montanino and G. Scioscia, Eur. Phys. J. C8 (1999) 609, hep-ex/9901012.

- 40) B. Baibussinov et al., (2009), arXiv:0909.0355.
- 41) V.N. Gavrin et al., (2010), arXiv:1006.2103.
- 42) S.K. Agarwalla and P. Huber, Phys. Lett. B696 (2011) 359, arXiv:1007.3228.
- 43) S.K. Agarwalla and R.S. Raghavan, (2010), arXiv:1011.4509.
- 44) J. Vergados, Y. Giomataris and Y. Novikov, (2011), arXiv:1103.5307.